Published in final edited form as:
Blood. 2011 September 29; 118(13): . doi:10.1182/blood-2010-09-311076.

Siglec-9 is a novel leukocyte ligand for Vascular Adhesion Protein-1 and can be utilized in PET-imaging of inflammation and cancer

Kristiina Aalto[#1], **Anu Autio**[#2], **Elina A. Kiss**[1], **Kati Elima**[1,3], **Yvonne Nymalm**[4], **Tibor Z. Veres**[1], **Fumiko Marttila-Ichihara**[1], **Heli Elovaara**[1], **Tiina Saanijoki**[2], **Paul R. Crocker**[5], **Mikael Maksimow**[1], **Eva Bligt**[4], **Tiina A. Salminen**[4], **Marko Salmi**[1,3,6], **Anne Roivainen**[2], and **Sirpa Jalkanen**[1,6]

[1]MediCity Research Laboratory and Department of Medical Microbiology and Immunology, University of Turku, Turku, Finland [2]Turku PET Centre, University of Turku, Turku, Finland [3]Department of Medical Biochemistry and Genetics, University of Turku, Turku, Finland [4]Structural Bioinformatics Laboratory, Department of Biosciences, Åbo Akademi University, Turku, Finland [5]The Wellcome Trust Biocentre, College of Life Sciences, University of Dundee, Dow Street, Dundee DD1 5EH, United Kingdom [6]National Institute of Public Health and Welfare, Turku, Finland

[#] These authors contributed equally to this work.

Abstract

Leukocyte migration to sites of inflammation is regulated by several endothelial adhesion molecules. Vascular Adhesion Protein-1 (VAP-1) is unique among the homing-associated molecules as it is both an enzyme that oxidizes primary amines and an adhesin. Although granulocytes can bind to endothelium via a VAP-1 dependent manner, the counter-receptor(s) on this leukocyte population is not known. Here we used a phage display approach and identified Siglec-9 as a candidate ligand on granulocytes. The binding between Siglec-9 and VAP-1 was confirmed by in vitro and ex vivo adhesion assays. The interaction sites between VAP-1 and Siglec-9 were identified by molecular modeling and confirmed by further binding assays with mutated proteins. Although the binding takes place in the enzymatic groove of VAP-1, it is only partially dependent on the enzymatic activity of VAP-1. In positron emission tomography the ^{68}Gallium- labeled peptide of Siglec-9 specifically detected VAP-1 in vasculature at sites of inflammation and cancer. Thus, the peptide binding to the enzymatic groove of VAP-1 can be used for imaging such conditions as inflammation and cancer.

Introduction

Leukocyte migration from the blood into the non-lymphoid tissues is a hallmark of inflammation. Several molecules on the endothelial cell surface and their counter-receptors

Correspondence: Prof. Sirpa Jalkanen, MediCity Research Laboratory, University of Turku, Tykistökatu 6 A, FIN-20520 Turku, Finland. Phone: +358 2 333 7007; fax: +358 2 333 7000; sirpa.jalkanen@utu.fi.

Authorship

Contribution: K.A., A.A., E.A.K., K.E., H.E., T.Z.V. and Y.N. performed the experiments and edited the manuscript, F.M.-I., E.B. and T.Saa performed the experiments, P.C. provided valuable reagents and edited the manuscript, M.M., M.S., A.R. and T.Sal designed the work and edited the manuscript, S.J. designed the work, analyzed data and wrote the manuscript.

Conflicts-of-interest disclosure: The authors declare no competing financial interests.

Europe PMC Funders Author Manuscripts

on vascular endothelium mediate a multistep adhesion cascade featuring tethering, rolling, activation, adhesion, crawling and transmigration phases.[1,2]

Vascular adhesion protein-1 (VAP-1/AOC3) is an endothelial cell molecule that is rapidly translocated from the intracellular storage granules to the endothelial cell surface upon inflammation. It contributes to several steps in the extravasation cascade and controls trafficking of lymphocytes, granulocytes and monocytes to sites of inflammation. VAP-1 has unique features distinct from other conventional adhesion molecules, because besides being an adhesin it is also an enzyme. It catalyzes oxidative deamination of primary amines and produces hydrogen peroxide, aldehyde and ammonium.[3] The end products of the enzymatic activity are highly potent inflammatory mediators and can upregulate other adhesion molecules such as E- and P-selectin, ICAM-1 and VCAM-1.[4,5]

We recently found the first lymphocyte ligand for VAP-1, Siglec-10.[6] It is expressed on B cells, monocytes and eosinophils but is absent from granulocytes.[7] However, VAP-1 is also involved in granulocyte migration to sites of inflammation. This has been demonstrated in studies with acute inflammation models (peritonitis, lung and air pouch inflammation) in mouse. In these studies significant reduction in granulocyte migration to sites of inflammation was obtained with a function blocking anti-VAP-1 antibody and a small molecular inhibitor against VAP-1.[8-10] Contribution of VAP-1 both at the rolling and transmigration steps during leukocyte extravasation has been demonstrated, and the enzymatic activity of VAP-1 seems to be important in these processes.[8,11,12] As granulocyte migration to sites of inflammation is mediated by VAP-1 we continued our search for granulocyte ligands for VAP-1. In this work we describe the discovery of Siglec-9 as a VAP-1 ligand on granulocytes and marked differences in Siglec-9/VAP-1 interaction in comparison to that between the earlier reported lymphocyte ligand, Siglec-10 and VAP-1. Furthermore, we demonstrate usefulness of a Siglec-9 peptide as an imaging tool in inflammation and cancer in positron emission tomography (PET).

Materials and Methods

Purified proteins, antibodies, reagents, synthetic peptides

Recombinant VAP-1 protein was purified from Chinese hamster ovary (CHO) cells stably transfected with the full-length human VAP-1 cDNA as described[6] and human placental lysate (with the permission of the local Ethical Committee). Monoclonal antibody TK-8-18 against human VAP-1 and the monoclonal and polyclonal antibodies against Siglec-9 and monoclonal anti-mouse VAP-1 antibody have been described.[7,9,13,14] Polyclonal rabbit anti-VAP-1 antibody was made against recombinant human VAP-1 but it recognizes also mouse VAP-1. Anti-human VAP-1 (Jg-2.10) and anti-mouse PV-1 (Meca-32) were gifts from E. Butcher, Stanford University. Monoclonal antibodies, 3G6 against chicken T cells,[15] Hermes-1 against human CD44[16] and HB-116 against human HLA A,B,C (clone MB40.5) from ATCC were used as negative control antibodies. The second stage antibodies and other reagents were purchased as follows: Alexa546 conjugated anti-rat IgG, Prolong Antifade Gold from Molecular probes (Eugene, Oregon, USA). FITC conjugated anti-rabbit-IgG and FITC-anti-rat IgG were from Sigma (St Louis, Missouri, USA). Alexa546-Streptavidin and CFSE were from Invitrogen and BM chemiluminescence ELISA substrate from Roche Applied Science (Basel, Switzerland) and synthetic peptides from NeoMPS (Strasbourg, France) and Almac Sciences (Elvingston Science Centre, Scotland, UK).

Phage display screening

Phage display screening with a cyclic peptide library containing CX8C decapeptides (where X is any amino acid) was performed as described.[17] Briefly, recombinant human VAP-1

(100 μg/mL in Tris buffered saline) was coated onto Nunc Maxisorp 96-well plates. The bound phages were eluted and used to infect K91kan *E. coli*. The amplified phages were used in three additional rounds of panning performed in the same manner. For colony sequencing primers 5′ and 3′ to the peptide insertion site of the phage were used: the forward primer was 5′-TAATACGACTCACTATAGGGCAAGCTGATTAACCGATACAAT-3′ and the reverse primer 5′-CCCTCATAGTTAGCGTAACGATCT-3′.

Cell lines and cell culture

CHO cells stably transfected with VAP-1, vector only and with Siglec-9 cDNAs have been described.[7,18] The enzymatically inactive mutant CHO-VAP-1Y471F has been generated as described in[8]. Also CHO cells stably transfected with mouse VAP-1[19] and mouse Siglec-E cDNAs were used.

Animals

Sprague-Dawley rats, wild type C57Black (WT), VAP-1 knockout (KO) and VAP-1 KOTG mice (mouse VAP-1 deficient mice expressing human VAP-1 as a transgene on endothelium under Tie-1 promoter[5]) were used under permissions of the Lab-Animal Care & Use Committee of the State Provincial Office of Southern Finland and in compliance with the Finnish laws relating to the conduct of animal experimentation.

Immunohistochemistry

Frozen sections of mesenteric lymph nodes of VAP-1 KO and VAP-1 KOTG mice were double-stained with anti-mouse PV-1 (Meca-32) detecting the blood vessels followed by FITC-conjugated anti-rat IgG and biotinylated anti-human VAP-1 (Jg-2.10) followed by Alexa546-Streptavidin. Also the tumors used for autoradiography were stained with polyclonal anti-VAP-1 and Meca-32 followed by FITC-conjugated anti-rabbit IgG and FITC-conjugated anti-rat IgG, respectively.

Adhesion assays

Assays with peptides and recombinant proteins—1) Recombinant VAP-1 and BSA (as a negative control) were immobilized on Nunc Maxisorp 96-well plates overnight at 4°C, blocked with PBS/3% BSA and incubated with biotinylated peptides (10 μg/mL) for 2 h at room temperature. Bound peptides were detected with HRP conjugated streptavidin and measured with a luminometer (Tecan Ultra, Tecan, Zürich, Switzerland).

2) Surface plasmon resonance (SPR) assays were done using a Biacore X (Biacore AB) as explained in detail in Supplemental Materials and Methods. Briefly, the recombinant or affinity purified human VAP-1 was immobilized on the CM5 sensor chip (Biacore AB) according to the manufacturer's instructions. First we tested the binding of Siglec-9 derived peptide (P1) to immobilized VAP-1. Each measurement was done twice to ensure the reproducibility of the observation. To test the specific binding of the peptide to VAP-1, the interaction of the peptide to the reference channel was subtracted from the VAP-1 curve.

To test qualitatively the role of two individual arginine residues of the peptide in the VAP-1/Siglec-9 interaction we measured the binding of four different cyclic peptides to immobilized VAP-1: wild type peptide (P1), peptide without arginines (P1_noArg), peptide without Arg284 (P1_noArg284) and peptide without Arg290 (P1_noArg290).

Assays with transfectants—1) CHO-VAP-1 and CHO mock cells were incubated with biotinylated Siglec-9 peptide for 20 min and after the washes the bound peptide was

detected with streptavidin-phycoerythrin. The cells were analyzed using FACSCalibur and Cellquest software.

2) CHO-VAP-1, CHO-VAP-1Y471F or CHO-mock cells were cultured to confluence on 96-well plates. After blocking the wells with PBS/1% BSA, 2×10^5 CFSE-labeled CHO-Siglec-9 or Siglec-E cells were added and incubated for 30 min at 37°C. After nine washes the adherence was quantified with a fluorometer (Tecan Infinite M200, Tecan, Zürich, Switzerland). The wells were imaged using Axiovert 200 M microscope with Hamamatsu ORCA camera.

Ex vivo frozen section assays—These binding assays were done as described[20] using lymph nodes from VAP-1 KO and VAP-1 KOTG mice. Percoll-purified human granulocytes were pre-treated with anti–Siglec-9 mAb and a negative control mAb (3G6) 10 μg/mL for 30 min before adding them onto the sections. The cells were let to bind to the vessels under rotating conditions for 30 min. Thereafter, the adherent cells were fixed with glutaraldehyde and the number of vessel-bound granulocytes was counted. The results are expressed as percentage of control binding. The number of granulocytes bound per venules in VAP-1 KOTG mice treated with the control mAb was chosen to define 100% binding. In addition, the number of venules supporting granulocyte binding was counted and is reported as mean percentage ± SEM.

In the second set of experiments human granulocytes from three donors were incubated for 2h with TNF-α (200 U/mL) or left untreated prior to the adhesion assays. Additional pre-treatments were done with anti-Siglec-9 or control antibodies for 30 min. Thereafter, granulocyte binding to vessels in human inflamed synovia was tested as explained above.

Intravital microscopy and image analysis

The procedures for visualizing blood vessels of the inflamed cremaster muscle have been described previously.[21,22] Briefly, VAP-1 KOTG mice were anaesthetized with an i.p. injection of ketamine and xylazine and 1.5 μg TNF-α was injected intrascrotally for inducing inflammation. After 4 hours, mice were anaesthetized again and a PE-10 polyethylene catheter (Becton Dickonson) was inserted into the left femoral artery. Subsequently, the right cremaster muscle was dissected free and pinned on a custom-built microscope stage. Percoll-purified human granulocytes were labeled with 20 μM 5-(and-6)-TAMRA SE (Invitrogen) and pretreated with anti-Siglec-9 mAb or with an isotype-matched, non-cytotoxic anti-HLA A, B, C control antibody produced using the respective hybridoma from ATCC (Cat# HB-116, clone MB40.5). PMNs from each donor were collected twice (on two different days) and were treated once with anti-Siglec-9 mAb and once with control mAb. Intravital epifluorescence video microscopy was performed using an Olympus BX50WI microscope equipped with stroboscopic illumination (Strobex 11360, Chadwick Helmuth, Mountain View, CA), a water immersion objective (20×/0.5) and a CDD video camera (Hamamatsu Photonics, Hamamatsu City, Japan). Multiple boluses of approx. 5-10 $\times 10^6$ cells in a volume of 50 μl PBS were injected via the arterial catheter during continuous video recording. Images of postcapillary venules with a diameter of 18 – 51 μm were typically recorded for 1-2 min after cell injection. Average centerline blood flow velocity of the observed vessels was measured with a commercial velocimeter (Circusoft Instrumentation, Hockessin, DE). Mean blood flow velocity and wall shear rate were calculated as described earlier.[22] The major microvascular parameters did not show any major differences between the two treatment groups (Supplemental Table 1). Interactions between PMNs and vessel wall were analyzed offline using Imaris 7.2.1. (Bitplane, Switzerland). The total as well as the rolling leukocyte flux were determined by manually counting the cells passing by a line drawn perpendicular to the venule axis in a frame-by-

frame manner. Rolling velocity was measured for at least 6 leukocytes randomly selected after each bolus injection. Adherent fraction was determined as the percentage of rolling cells that arrested on the venular wall for ≥ 30 s.

Inductions and FACS stainings

Red cells were lysed from the whole blood and the remaining leukocytes of four healthy volunteers were treated with FMLP (0.5 and 5 μg/mL for 5 min and 2 h), TNF-α (10 and 200 U/mL 2 h) or LPS (10 and 100ng/mL for 2 h). Untreated cells served as controls. Siglec-9 expression was analyzed by monoclonal anti-Siglec-9 antibody and 3G6 was a control. The second stage antibody was Alexa546-conjugated anti-mouse IgG. In double staining experiments the monocytes were detected by FITC-anti-CD14 and granulocytes by FITC-anti-CD66b. The cells were analyzed using FACSCalibur and Cellquest software.

Modeling and docking simulation

The structural model of the second Siglec-9 C2 domain was made using the crystal structure of the first Siglec-5 C2 domain (pdb code: 2zg2).[23] Ten models were generated with Modeller[24] and the model with the lowest objective function was chosen. The sequence alignments were performed using MALIGN and MALFORM[25] within the Bodil visualization and modeling package.[26] The cyclic peptide CARLSLSWRGLTLCPSK containing residues **283-297** from Siglec-9 was generated using SYBYL® 7.3 (Tripos Inc., St. Louis, Missouri, USA). Since the peptide contains two arginines, which could bind to topaquinone, each of them were covalently bound to topaquinone in a VAP-1 structure[27] (pdb code: 1us1) in separate docking studies. Ten dockings with Arg284 or Arg290 in the peptide covalently bound to the N5 atom of topaquinone in an active conformation, were made using GOLD 3.2.[28,29] The arginines in the peptide were also mutated one by one and the mutant peptides with only one arginine were similarly docked into VAP-1. Leu469 and Thr212 were made flexible during docking to allow access to the active site. In addition, Asp446 from the other monomer and near the catalytic site was flexible during docking. Since the dockings with Arg284 bound to topaquinone gave the highest fitness value derived by GOLD, this peptide-VAP-1 model was chosen for further analysis. Figure 4 was created with PYMOL.

PET studies

A cyclic peptide, CARLSLSWRGLTLCPSK, having 8-amino-3,6-diooxaoctanoyl linker (PEG derivative) between 1,4,7,10-tetraazacyclododecane-N,N′,N″,N‴-tetraacetic acid (DOTA) and peptide was labeled with ^{68}Ga as previously described.[30] Radiochemical purity was determined by reversed-phase HPLC.

Rats with sterile inflammation—Sprague-Dawley rats were subcutaneously injected with turpentine oil (Sigma-Aldrich) into the upper neck area and inflammation was allowed to develop for 24 h prior to PET study. The whole-body distribution kinetics and inflammation imaging of intravenously (i.v) administered ^{68}Ga-DOTA-peptide (18.4 ± 3.1 MBq) were evaluated using a High Resolution Research Tomograph (CPS Innovations). Blood samples were drawn during PET imaging. Data acquired for 60 min in a list mode were iteratively reconstructed with the ordered-subsets expectation maximization 3D algorithm (OSEM3D). Quantitative analysis was performed by drawing regions of interest (ROI) in the brain, heart, inflammation, kidney, liver, lung, muscle and urinary bladder areas. The average radioactivity concentration in the ROI (kBq/mL) was used for further analyses. The uptake was reported as standardized uptake value (SUV), which was calculated as the radioactivity concentration of the ROI divided by the relative injected radioactivity expressed per animal body weight. The radioactivity remaining in the tail was

also compensated. Bio-kinetic curves, representing radioactivity concentration in the organ of interest versus time after injection, were determined accordingly.

After PET imaging animals were killed and samples of blood, urine and various organs were excised, weighed, and measured for radioactivity using a gamma counter. The radioactivity uptake was reported as SUV.

Mice with tumor xenografts—B16 melanoma cells were injected into neck area in PET imaging studies and in abdominal area for autoradiograph studies as a model for solid tumors. The mice were used 11 days after the inoculation of the tumors. The tumor uptake kinetics and whole-body distribution of i.v. injected ^{68}Ga-DOTA-peptide (7.8 ± 2.3 MBq) were evaluated in mice bearing the melanoma xenograft. Dynamic PET imaging for 60 min was performed using Inveon Multimodality scanner (Siemens) and reconstructed with OSEM2D. Specificity of ^{68}Ga-DOTA-peptide uptake was verified in competitive experiments with 500-fold molar excess of unlabeled DOTA-peptide. The results were expressed as SUV and verified by ex vivo measurements as described above.

Distribution of radioactivity in tumor was also studied with digital autoradiography of cryosections. Mice were i.v injected with ^{68}Ga-DOTA-peptide (3.0 ± 0.4 MBq) and killed 15 min later. The autoradiographs were analyzed for photostimulated luminescence per unit area (PSL/mm^2). ROIs were drawn on VAP-1 positive and VAP-1 negative areas according to immunohistochemical staining of adjacent sections. Background area count densities were subtracted from the image data and uptake values were normalized against the control site (muscle).

Mice with inflammation—Skin inflammation was induced with 4 drops of 5% (w/v) dinitrochlorobenzene (1-chloro-2,4-dinitrobenzene, DNCB, Sigma) in acetone applied onto the right ear of VAP-1 KO and VAP-1 KOTG mice one day before the PET imaging. The inflammation uptake kinetics and whole-body distribution of i.v. injected ^{68}Ga-DOTA-peptide were evaluated in KO (7.4 ± 1.8 MBq) and KOTG (7.5 ± 3.0 MBq) mice. Dynamic PET imaging for 30 min was performed using Inveon Multimodality scanner (Siemens) and reconstructed with OSEM2D. The results are expressed as SUV and verified by ex vivo measurements as described above.

Statistical analyses

Student's *t* test (unpaired, 2-tailed) was used to compare numerical variables between two groups.

Results

Siglec-9 binds to VAP-1

A CX_8C phage peptide library was used to screen for potential ligands of VAP-1. After four rounds of panning using recombinant VAP-1 as a bait we obtained a 400-fold enrichment of phages bound to VAP-1 in comparison to the control (BSA coated wells). Of the 23 randomly selected phages sequenced, nineteen gave a sequence shown in Figure 1A. Database searches with the sequence derived from the phage clones revealed similarities to the amino acid sequence of Siglec-9 (residues 289 – 295, Figure 1A). In the binding assays the phage peptide bound selectively to recombinant VAP-1 (Figure 1A).

Additional adhesion assays were performed to demonstrate binding between Siglec-9 and VAP-1 expressing cells. In these studies the Siglec-9 derived peptide adhered more efficiently to VAP-1 transfectants than to the mock transfected controls not expressing

VAP-1 (Figure 1B). For further confirmation, the interaction between cells expressing VAP-1 and cells expressing Siglec-9 was studied. The results were consistent with those of the previous experiments and showed VAP-1-Siglec-9 dependent adhesion of the cells expressing these molecules (Figure 1C).

Granulocytes use Siglec-9 for binding to endothelial VAP-1

All peripheral blood granulocytes are Siglec-9 positive (Figure 2A). To test whether expression of Siglec-9 can be up-regulated by inflammatory mediators, we used formyl-methyl-leucine-phenylalanine (FMLP), tumor necrosis factor-α (TNF-α), and lipopolysaccharide (LPS) in the induction experiments. FMLP slightly up-regulated Siglec-9 expression already after 5 min and further up-regulation was seen after 2 h. Also LPS and TNF-α caused a significant up-regulation of Siglec-9 after 2 h (Figure 2B). Comparable up-regulation was also seen on CD14 positive monocytes (data not shown).

Next we analyzed, whether granulocytes can bind endothelial VAP-1 in a Siglec-9 dependent manner. We tested granulocyte binding to lymph node vasculature of both VAP-1 knockout (KO) mice and transgenic VAP-1 KO mice expressing human VAP-1 on endothelium (KOTG)[5] in ex vivo frozen section adhesion assays. This setting allowed us to measure binding between Siglec-9 and VAP-1 without the theoretical possibility that Siglec-9 adheres to another (unknown) endothelial cell molecule and VAP-1 binds to another (unknown) leukocyte ligand that is impossible to discriminate from the specific binding by using frozen sections from wild type murine or human lymph nodes. Expression of human VAP-1 in KOTG lymph node vasculature is shown in Figure 2C. The binding assays demonstrated that the vessels expressing human VAP-1 mediates significantly better adherence of granulocytes than the vessels in KO lymph nodes. Moreover, the binding was largely mediated by Siglec-9 as anti-Siglec-9 antibody significantly reduced number of granulocytes adhering to KOTG vessels but did not have any inhibitory effect in KO lymph nodes (Figure 2D). 76.3 ± 4.7% of the KOTG vessels (320 counted) treated with the negative control antibody supported granulocyte binding, whereas the corresponding percentage was 15.3 ± 2.1% after the anti-Siglec-9 antibody treatment (335 vessels counted; $P = 0.0006$). These experiments demonstrate that the interaction between Siglec-9 and VAP-1 can occur upon the binding of granulocytes to the vessel wall.

We also tested, whether TNF-α induced upregulation of Siglec-9 enhances binding of human granulocytes to vessels in inflamed synovium. In these experiments, TNF-a treatment significantly increased granulocyte binding to synovial vasculature and this increase could be inhibited by antibody-blocking of Siglec-9 (Figure 2E).

We further wanted to explore, whether Siglec-9 is required for the interaction of granulocytes with the inflamed endothelium *in vivo*. Therefore, we performed intravital microscopic experiments to visualize the behavior of human granulocytes within the inflamed vasculature of VAP-1 KOTG mice. To avoid trapping of the injected cells in the lung, PMNs were injected into the femoral artery during continuous observation of blood vessels in the contralateral cremaster muscle as described earlier.[31] To address the role of Siglec-9 expressed on the surface of human PMNs, the cells were pre-treated either with anti-Siglec-9 mAb or with a control class-matched binding mAb (directed against HLA A, B, C). Staining of PMNs with anti-Siglec-9 mAb or with the control anti-HLA mAb resulted in a similar fluorescence intensity level observed using FACS analysis (results not shown). This ensures that the Fc-mediated clearance of human PMNs from the circulation would occur at the same rate when treated with the anti-Siglec-9 mAb or with the control mAb.

Immediately after their injection, numerous rolling granulocytes were detected along the inflamed venules, together with a few firmly adherent cells (Supplementary Video 1).

Pretreatment of granulocytes with anti-Siglec-9 mAb prior to their transfer resulted in a mild decrease in the rolling fraction (which is expressed as a percentage of rolling cells within the total number of cells, which travelled through the vessel during the period of observation) as shown in Figure 2F. However, the velocity of the rolling cells (Figure 2G) as well as the adherent fraction (representing the percentage of the rolling cells that arrested on the vessel wall for ≥ 30 s) were not affected by the antibody treatment (Figure 2H). These results suggest that Siglec-9 contributes to the initiation of the rolling step in the extravasation cascade, but does not affect overall firm adhesion in this experimental system.

Siglec-9 binds to the enzymatic groove of VAP-1

Next we investigated, whether the interaction between Siglec-9 and VAP-1 involves enzymatic activity. This was tested in cell-mediated binding assays using the transfectants expressing the wild type VAP-1 and the enzymatically inactive VAP-1 mutant, in which tyrosine 471, the precursor of topaquinone, has been mutated to phenylalanine. These assays revealed that binding of cells expressing Siglec-9 to the cells with the inactive mutant of VAP-1 on the surface was significantly reduced in comparison to the cells expressing the wild type VAP-1. However, the enzymatic inactivation did not reduce the binding to the background level suggesting contribution of some other epitopes (Figure 3A-B).

Based on the Siglec-9 sequence the two arginines (Arg284 and Arg290) in the Siglec-9 peptide are the primary candidates to interact with the topaquinone of VAP-1. We used surface plasmon resonance (SPR) to assay the binding of wild type and mutated Siglec-9-like peptides to recombinant VAP-1 and affinity purified VAP-1. A cyclic peptide with a full match to the corresponding Siglec-9 amino acid sequence (CARLSLSWRGLTLCPS, containing residues 283-297 from Siglec-9) bound to recombinant VAP-1 (Figure 3C). Instead, the mutated Siglec-9 peptide, in which both arginines were mutated to alanines failed to bind recombinant VAP-1 in Biacore assays (data not shown). Next, we mutated the Arg284 and Arg290 separately. Both mutations reduced binding: Arg284 seemed to be more critical as the binding was dramatically reduced (66 ± 7%, n = 3, $P = 0.04$) subsequent to its mutation. Binding of the peptide with Arg290 mutation was also diminished in comparison to the wild type peptide although to a slightly lesser extent (42 ± 14%, n = 3, $P = 0.05$) (Figure 3D).

To test, whether the Siglec-9 peptide fits to the enzymatic groove of VAP-1 we performed docking studies utilizing the crystallographic structure of VAP-1. The results are in accordance with the binding studies since the peptide fits to the enzymatic groove of VAP-1 best when Arg284 is covalently bound to topaquinone (Figure 4).

Taken together, these data suggest that Siglec-9 binds to the enzymatic groove of VAP-1 and arginine at the position 284 in Siglec-9 is the binding partner in the enzyme activity-dependent part of the binding. However, also Arg290 seems to contribute to the interaction by binding to another site in the groove.

In this context it is important to note that the corresponding mouse molecule for human Siglec-9 is Siglec-E that does not have the required arginines for binding to VAP-1 (Supplemental Figure 1). We also confirmed the importance of the arginine residues in the experiments, in which binding of CHO-cells transfected with Siglec-E or mock constructs was measured to CHO-cells transfected with mouse VAP-1 and no VAP-1-Siglec-E mediated adhesion was detected (Supplemental Figure 1).

Siglec-9 peptide can be used for in vivo imaging

VAP-1 expression is induced at sites of inflammation and in neo-vasculature of certain cancers.[21,32] We therefore wanted to analyze, whether the Siglec-9 peptide identified here

can be used to image inflammation and tumors expressing VAP-1 on the vasculature. We first chose a turpentine inflammation model in rat and continued with a cancer model in mouse. The latter model also provided an additional specificity control as VAP-1 KO mice were available for the studies. ^{68}Gallium labeled DOTA-conjugated Siglec-9 peptide was used as an imaging agent. ^{68}Ga-DOTA-peptide quickly and preferentially accumulated at the sites of inflammation (5-10 min) in comparison to the muscle (Figure 5), indicating that the peptide detects the inflammation. Excess of the peptide was eliminated rapidly via kidneys to the urinary bladder. We then tested, whether the peptide is able to detect tumor and whether the detection is specific. Also in this case the peptide accumulated at the tumor site and the accumulation of the radioactive peptide could be inhibited with 500x cold peptide (Figure 6A) demonstrating the specificity of the peptide. Comparable results were seen in the assays with the control peptide in the rat inflammation model (data not shown). The cold peptide could compete the radioactive peptide binding in all organs to the levels detected in the VAP-1 knockout mice except in the kidneys (Table 1). The kidneys are the elimination routes of the peptide, therefore showing high level of radioactivity in all mouse groups (Table 1). In the tumor bearing mice, the radioactivity concentrated in the periphery of the tumor (Figure 6B-C). It is consistent with the finding that VAP-1 expression is also highest in these areas (Figure 6D-E). VAP-1 is present on a subset of vessels as can be seen when the same tumor is stained with an anti-PV-1 antibody (Figure 6F), which is a prototype marker for blood vessels.[33] Thus, these results indicate that the radioactive peptide specifically detects VAP-1 positive vessels.

We further tested, whether the ^{68}Gallium labeled DOTA-conjugated Siglec-9 peptide could be used to image inflammation in the mouse. For these experiments we used VAP-1 KO mice and KOTG mice expressing human VAP-1 on the endothelium. The model chosen was a skin inflammation. As demonstrated in Supplemental Table 2, the peptide detects human VAP-1 in many organs realized as higher signals than in KO mice. Moreover, the peptide was able to detect inflammation in the mouse as well (Supplemental Figure 2).

Discussion

VAP-1 mediates granulocyte binding to endothelium and their traffic to sites of inflammation[9] suggesting existence of a granulocyte ligand(s) for VAP-1. Despite numerous attempts such a ligand(s) has so far remained unidentified. One reason may be the inherently weak and transient interaction between VAP-1 and its ligand within the enzymatic groove of VAP-1. The discovery of Siglec-9 being a ligand for VAP-1 on granulocytes increases our understanding of the ecto-enzymatic mechanisms in the leukocyte adhesion cascade.

We found that the expression of Siglec-9 was rapidly up-regulated on the leukocyte surface after inflammatory stimuli. A slight up-regulation was already seen after 5 min with FMLP and the increase was roughly two-fold after 2 h when measured as mean fluorescence intensities. These findings suggest that the up-regulation does not need new protein synthesis. The rapid translocation of VAP-1 from intracellular granules to endothelial cell surface upon inflammation and the up-regulation of Siglec-9 on granulocytes and monocytes by inflammatory mediators such as LPS and TNF-α may significantly facilitate leukocyte trafficking to sites of inflammation and infection in vivo. As a matter of fact, we could experimentally show that TNF-α treatment increased Siglec-9 mediated granulocyte binding to vasculature in inflamed human synovium.

Siglec-E, the mouse orthologue /homologue of human Siglec-9, does not have the necessary arginines to bind to VAP-1 preventing us to study the role of Siglec-E-VAP-1 interaction in the mouse system. Therefore, we constructed an intravital set-up by injecting human granulocytes into the mice expressing human VAP-1 on endothelium. Although this system

has its inherent limitations, it allowed us to conclude that Siglec-9 is involved in the rolling step of the adhesion cascade. This fits well to the reported involvement of VAP-1 in the rolling step and the rapid and transient (0.3 seconds) Schiff-based interactions between the primary amine oxidases and their substrates.[3] However, it is still theoretically possible that in our experimental setting Siglec-9 interacts with a VAP-1 independent ligand on the endothelium. However, this alternative is not very likely in the light of the documented interaction between Siglec-9 and VAP-1 in the *in vitro* frozen section binding assays (Figure 2D).

As VAP-1 is an enzyme and its enzymatic activity is central in granulocyte-endothelial cell interaction,[8] it seemed highly likely that the interaction between VAP-1 and Siglec-9 also involves enzymatic activity. The narrow channel of the enzymatic groove of VAP-1 sets strict requirements for the possible ligands. Similarly as the lymphocyte ligand Siglec-10,[6] the Siglec-9 derived peptide fulfills the conformational criteria. We formally tested the contribution of the enzymatic activity in the in vitro binding assays with an enzymatically inactive VAP-1 mutant lacking the important tyrosine and expressing phenylalanine instead. This inactive mutant bound less efficiently than the wild type peptide to Siglec-9 demonstrating the importance of the topaquinone (modified from the tyrosine residue) in the binding. Based on the docking results and further binding studies with the mutated Siglec-9 peptides, Arg284 in Siglec-9 is the amino acid residue interacting with topaquinone. In the model of Siglec-9, Arg284 is located on the surface of the molecule and freely accessible for its counter-receptor. Interestingly, the interaction between Siglec-9 and VAP-1 differs from that between Siglec-10 and VAP-1. Siglec-10 has only one arginine in the binding peptide and the interaction is completely dependent on the enzymatic activity of VAP-1 (tyrosine 471) and Arg293 in Siglec-10.[6] In the case of Siglec-9, however, efficient binding seems to require two arginines (Arg284 and Arg290), one binding to topaquinone and the other one is facilitating interaction by binding to another site in the groove. This is well in line with the finding that enzymatically inactive VAP-1 can still bind to Siglec-9 although less efficiently than the wild type VAP-1. Mapping of these interacting sites on Siglec-9 may now facilitate design of better drugs/inhibitors to prevent harmful cell trafficking.

Imaging of inflammation and cancer with antibodies against endothelial adhesion molecules as targets has been shown to be a feasible option in animal models and also in human diseases.[34-37] However, better imaging tools are urgently needed for clinical medicine. Now we show that inflammation and cancer can be detected by using a VAP-1 binding peptide. VAP-1 is an optimal imaging target as in normal conditions it is mainly absent from the endothelial cell surface and is stored within intracellular granules. From there it is rapidly translocated to the endothelial cell surface in inflammation and certain cancers and thus, leaves normal endothelium non-targeted during imaging. On the other hand, an inherent advantage of the peptide is that it is rather quickly degraded/eliminated from plasma allowing a rapid imaging schedule. Therefore, combination of VAP-1 as a target and its natural binding structure as an imaging tool provides a theoretically optimal setting. In this work, we showed the proof of concept for this idea, and further studies will test its usability in patients.

Supplementary Material

Refer to Web version on PubMed Central for supplementary material.

Acknowledgments

We acknowledge Anne Sovikoski-Georgieva for secretarial help and Mark Johnson for the excellent computing facilities at Åbo Akademi University.

This work was supported by the Finnish Academy (S.J., M.S., A.R., T.A.S., H.E.), the Turku University Hospital (A.A., A.R.), the Finnish Cancer Foundation (S.J.), the Sigrid Juselius Foundation (S.J., M.S., T.A.S.) Arvo and Inkeri Suominen Foundation (S.J.), the National Graduate Schools in Informational and Structural Biology (E.B.), Drug Discovery (A.A), and Nanoscience (K.A., E.A.K.), the Research Institute of the Åbo Akademi Foundation (T.A.S.), Tor, Joe and Pentti Borg's Foundation (T.A.S.), the Wellcome Trust WT081882 (P.R.C.) and Medicinska Understödsföreningen Liv och Hälsa (Y.N.).

References

1. Butcher EC. Leukocyte-endothelial cell recognition: three (or more) steps to specificity and diversity. Cell. 1991; 67(6):1033–1036. [PubMed: 1760836]
2. Zarbock A, Ley K. Mechanisms and consequences of neutrophil interaction with the endothelium. Am J Pathol. 2008; 172(1):1–7. [PubMed: 18079440]
3. Salmi M, Jalkanen S. Cell-surface enzymes in control of leukocyte trafficking. Nat Rev Immunol. 2005; 5(10):760–771. [PubMed: 16200079]
4. Lalor PF, Sun PJ, Weston CJ, Martin-Santos A, Wakelam MJ, Adams DH. Activation of vascular adhesion protein-1 on liver endothelium results in an NF-kappaB-dependent increase in lymphocyte adhesion. Hepatology. 2007; 45(2):465–474. [PubMed: 17256751]
5. Jalkanen S, Karikoski M, Mercier N, et al. The oxidase activity of vascular adhesion protein-1 (VAP-1) induces endothelial E- and P-selectins and leukocyte binding. Blood. 2007; 110(6):1864–1870. [PubMed: 17548577]
6. Kivi E, Elima K, Aalto K, et al. Human Siglec-10 can bind to vascular adhesion protein-1 and serves as its substrate. Blood. 2009; 114(26):5385–5392. [PubMed: 19861682]
7. Munday J, Kerr S, Ni J, et al. Identification, characterization and leucocyte expression of Siglec-10, a novel human sialic acid-binding receptor. Biochem J. 2001; 355(Pt 2):489–497. [PubMed: 11284738]
8. Koskinen K, Vainio PJ, Smith DJ, et al. Granulocyte transmigration through the endothelium is regulated by the oxidase activity of vascular adhesion protein-1 (VAP-1). Blood. 2004; 103(9):3388–3395. [PubMed: 14726375]
9. Merinen M, Irjala H, Salmi M, Jaakkola I, Hanninen A, Jalkanen S. Vascular adhesion protein-1 is involved in both acute and chronic inflammation in the mouse. Am J Pathol. 2005; 166(3):793–800. [PubMed: 15743791]
10. O'Rourke AM, Wang EY, Miller A, et al. Anti-inflammatory effects of LJP 1586 [Z-3-fluoro-2-(4-methoxybenzyl)allylamine hydrochloride], an amine-based inhibitor of semicarbazide-sensitive amine oxidase activity. J Pharmacol Exp Ther. 2008; 324(2):867–875. [PubMed: 17993604]
11. Bonder CS, Norman MU, Swain MG, et al. Rules of recruitment for Th1 and Th2 lymphocytes in inflamed liver: a role for alpha-4 integrin and vascular adhesion protein-1. Immunity. 2005; 23(2):153–163. [PubMed: 16111634]
12. Tohka S, Laukkanen M, Jalkanen S, Salmi M. Vascular adhesion protein 1 (VAP-1) functions as a molecular brake during granulocyte rolling and mediates recruitment in vivo. FASEB J. 2001; 15(2):373–382. [PubMed: 11156953]
13. Kurkijarvi R, Adams DH, Leino R, Mottonen T, Jalkanen S, Salmi M. Circulating form of human vascular adhesion protein-1 (VAP-1): increased serum levels in inflammatory liver diseases. J Immunol. 1998; 161(3):1549–1557. [PubMed: 9686623]
14. Salmi M, Koskinen K, Henttinen T, Elima K, Jalkanen S. CLEVER-1 mediates lymphocyte transmigration through vascular and lymphatic endothelium. Blood. 2004; 104(13):3849–3857. [PubMed: 15297319]
15. Salmi M, Jalkanen S. A 90-kilodalton endothelial cell molecule mediating lymphocyte binding in humans. Science. 1992; 257(5075):1407–1409. [PubMed: 1529341]
16. Jalkanen ST, Bargatze RF, Herron LR, Butcher EC. A lymphoid cell surface glycoprotein involved in endothelial cell recognition and lymphocyte homing in man. Eur J Immunol. 1986; 16(10):1195–1202. [PubMed: 2429846]
17. Koivunen E, Arap W, Rajotte D, Lahdenranta J, Pasqualini R. Identification of receptor ligands with phage display peptide libraries. J Nucl Med. 1999; 40(5):883–888. [PubMed: 10319765]

18. Salmi M, Tohka S, Jalkanen S. Human vascular adhesion protein-1 (VAP-1) plays a critical role in lymphocyte-endothelial cell adhesion cascade under shear. Circ Res. 2000; 86(12):1245–1251. [PubMed: 10864915]
19. Bono P, Jalkanen S, Salmi M. Mouse vascular adhesion protein 1 is a sialoglycoprotein with enzymatic activity and is induced in diabetic insulitis. Am J Pathol. 1999; 155(5):1613–1624. [PubMed: 10550318]
20. Salmi M, Jalkanen S. Human leukocyte subpopulations from inflamed gut bind to joint vasculature using distinct sets of adhesion molecules. J Immunol. 2001; 166(7):4650–4657. [PubMed: 11254724]
21. Stolen CM, Marttila-Ichihara F, Koskinen K, et al. Absence of the endothelial oxidase AOC3 leads to abnormal leukocyte traffic in vivo. Immunity. 2005; 22(1):105–115. [PubMed: 15664163]
22. Dunne JL, Collins RG, Beaudet AL, Ballantyne CM, Ley K. Mac-1, but not LFA-1, uses intercellular adhesion molecule-1 to mediate slow leukocyte rolling in TNF-alpha-induced inflammation. J Immunol. 2003; 171(11):6105–6111. [PubMed: 14634125]
23. Zhuravleva MA, Trandem K, Sun PD. Structural implications of Siglec-5-mediated sialoglycan recognition. J Mol Biol. 2008; 375(2):437–447. [PubMed: 18022638]
24. Sali A, Blundell TL. Comparative protein modelling by satisfaction of spatial restraints. J Mol Biol. 1993; 234(3):779–815. [PubMed: 8254673]
25. Johnson MS, Overington JP. A structural basis for sequence comparisons. An evaluation of scoring methodologies. J Mol Biol. 1993; 233(4):716–738. [PubMed: 8411177]
26. Lehtonen JV, Still DJ, Rantanen VV, et al. BODIL: a molecular modeling environment for structure-function analysis and drug design. J Comput Aided Mol Des. 2004; 18(6):401–419. [PubMed: 15663001]
27. Airenne TT, Nymalm Y, Kidron H, et al. Crystal structure of the human vascular adhesion protein-1: unique structural features with functional implications. Protein Sci. 2005; 14(8):1964–1974. [PubMed: 16046623]
28. Jones G, Willett P, Glen RC. Molecular recognition of receptor sites using a genetic algorithm with a description of desolvation. J Mol Biol. 1995; 245(1):43–53. [PubMed: 7823319]
29. Jones G, Willett P, Glen RC, Leach AR, Taylor R. Development and validation of a genetic algorithm for flexible docking. J Mol Biol. 1997; 267(3):727–748. [PubMed: 9126849]
30. Ujula T, Salomaki S, Virsu P, et al. Synthesis, 68Ga labeling and preliminary evaluation of DOTA peptide binding vascular adhesion protein-1: a potential PET imaging agent for diagnosing osteomyelitis. Nuclear Medicine and Biology. 2009; 36(6):631–641. [PubMed: 19647169]
31. Goodarzi K, Goodarzi M, Tager AM, Luster AD, von Andrian UH. Leukotriene B4 and BLT1 control cytotoxic effector T cell recruitment to inflamed tissues. Nat Immunol. 2003; 4(10):965–973. [PubMed: 12949533]
32. Marttila-Ichihara F, Auvinen K, Elima K, Jalkanen S, Salmi M. Vascular adhesion protein-1 enhances tumor growth by supporting recruitment of Gr-1+CD11b+ myeloid cells into tumors. Cancer Research. 2009; 69(19):7875–7883. [PubMed: 19789345]
33. Keuschnigg J, Henttinen T, Auvinen K, Karikoski M, Salmi M, Jalkanen S. The prototype endothelial marker PAL-E is a leukocyte trafficking molecule. Blood. 2009; 114(2):478–484. [PubMed: 19420356]
34. Jaakkola K, Nikula T, Holopainen R, et al. In vivo detection of vascular adhesion protein-1 in experimental inflammation. Am J Pathol. 2000; 157(2):463–471. [PubMed: 10934150]
35. Fonsatti E, Jekunen A, Kairemo K, et al. Endoglin is a suitable target for efficient imaging of solid tumors: in vivo evidence in a canine mammary carcinoma model. Clin Cancer Res. 2000; 6(5): 2037–2043. [PubMed: 10815930]
36. Garrood T, Blades M, Haskard DO, Mather S, Pitzalis C. A novel model for the pre-clinical imaging of inflamed human synovial vasculature. Rheumatology (Oxford). 2009; 48(8):926–931. [PubMed: 19491304]
37. Malviya G, Conti F, Chianelli M, Scopinaro F, Dierckx RA, Signore A. Molecular imaging of rheumatoid arthritis by radiolabelled monoclonal antibodies: new imaging strategies to guide molecular therapies. Eur J Nucl Med Mol Imaging. 2010; 37(2):386–398. [PubMed: 19777175]

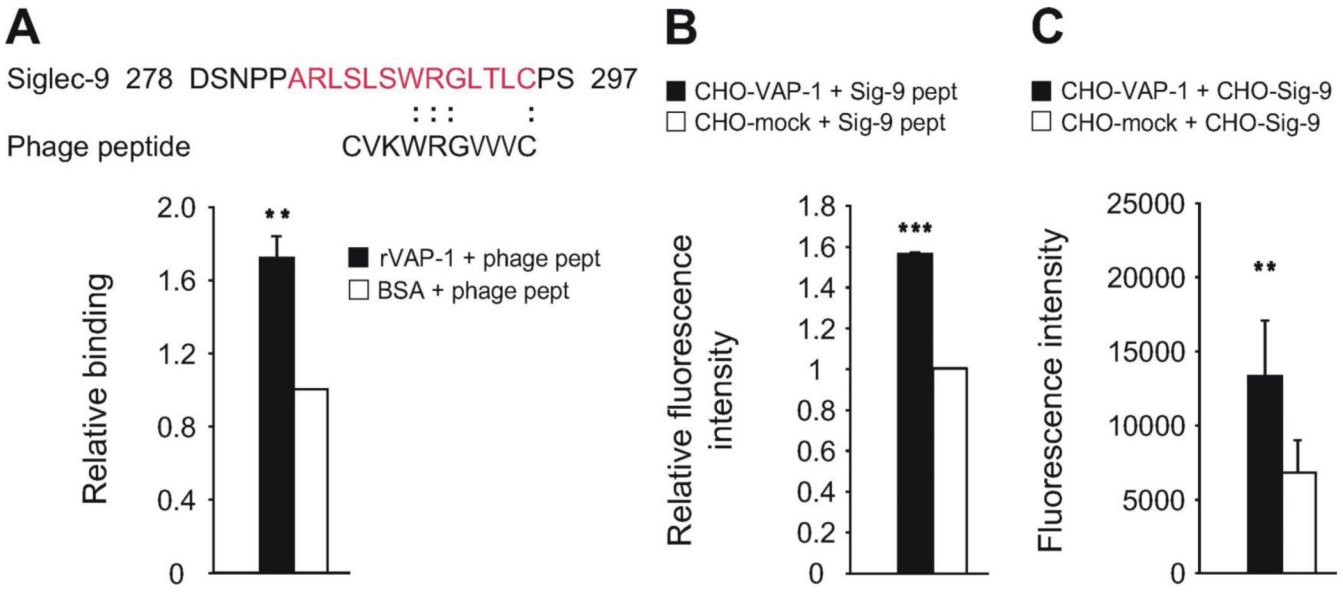

Figure 1. Siglec-9 interacts with VAP-1

(A) The amino acid sequence of the enriched phage clone, the corresponding region of Siglec-9 and the adhesion of the phage peptide to recombinant VAP-1 (rVAP-1 100 ng/well) measured using EIA. The results are mean ± SEM from three separate experiments and triplicate wells in each experiment. (B) Binding of the Siglec-9 peptide (Sig-9 pept marked red in A) to CHO-VAP-1 transfectants and CHO-mock controls. The results are presented as relative fluorescence intensity and are mean ± SEM from two separate experiments each having triplicate wells. (C) Binding of CFSE labeled Siglec-9 transfectants to CHO cells expressing VAP-1 and mock controls. The results are mean ± SEM of fluorescent intensities measured by fluorometer from seven separate experiments each having duplicate wells. $^{**}P < 0.01$; $^{***}P < 0.001$.

Europe PMC Funders Author Manuscripts

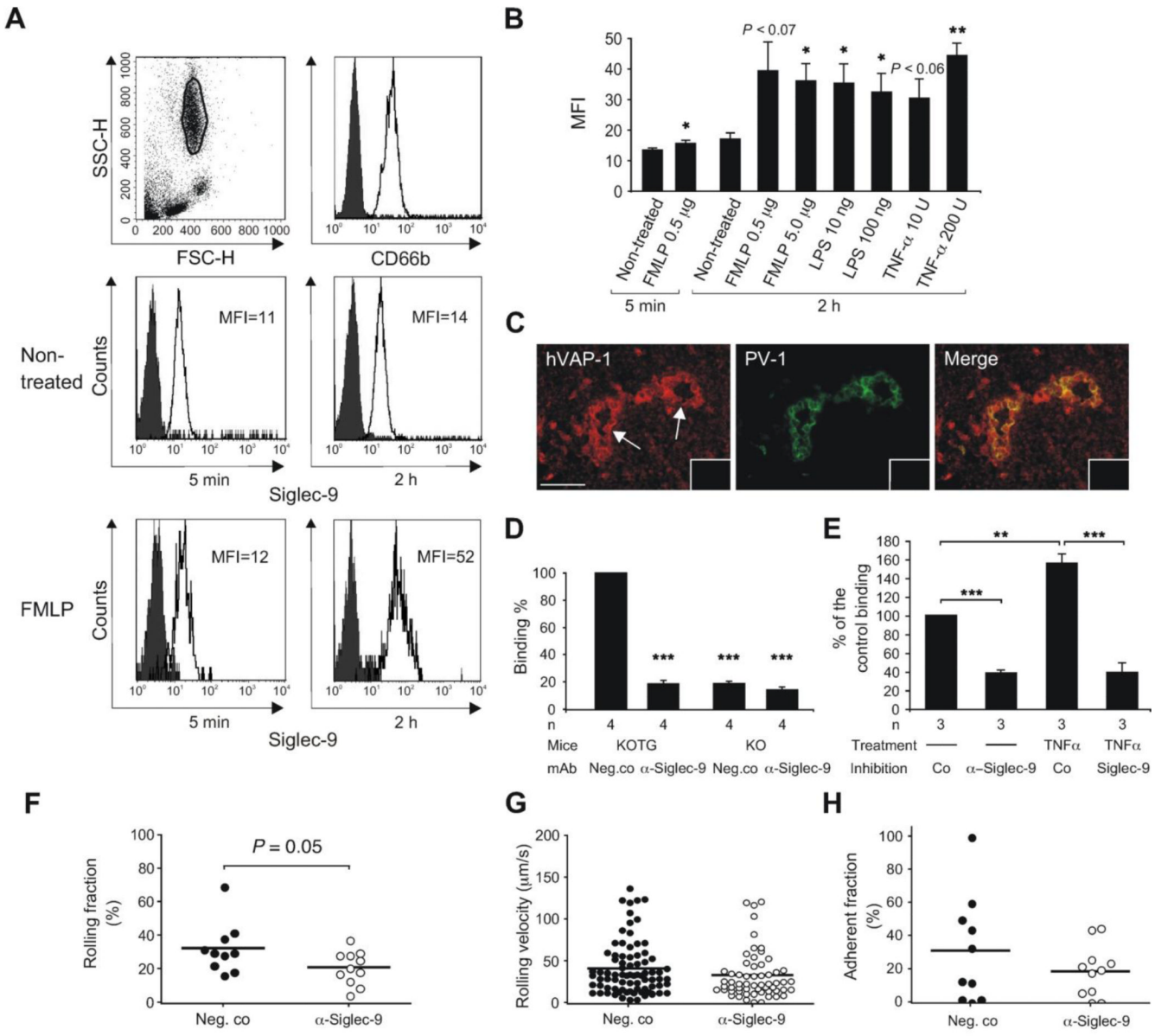

Figure 2. Siglec-9 positive leukocytes bind to vessels using VAP-1

(A) Expression of Siglec-9 on granulocytes used for ex vivo binding assays. FACS histograms of CD66b and Siglec-9 expression are shown with and without incubation in FMLP containing medium. Histograms with the negative control antibody are black. (B) Combined results of the induction experiments (mean ± SEM, n = 4) with FMLP, LPS and TNF-α (values indicated /mL). (C) Expression of human VAP-1 (hVAP-1) is detected with biotinylated Jg.2-10 **(**red, left panel**)**. Expression of PV-1 positive vessels in mesenteric lymph node vasculature of KOTG is detected by Meca-32 antibody (green, middle panel). High endothelial venules are pointed out by arrow. The merge of the panels is on the right. Stainings with a negative control antibody are shown in the insets. Scale bar 50 μm. (D) Ex vivo frozen section binding assays were used to analyze granulocyte binding to vessels in mesenteric lymph nodes obtained from VAP-1 KO and VAP-1 KOTG mice. The function of Siglec-9 was blocked by incubating the cells with anti-Siglec-9 antibody prior to the assay. (E) Granulocyte binding to inflamed synovial vessels. The granulocytes were pre-treated

Europe PMC Funders Author Manuscripts

with TNF-α and with anti-Siglec-9 and control antibodies as indicated. In D and E the results are shown as percentage of control binding (number of KOTG vessel-bound or synovial vessel-bound granulocytes incubated with a non-blocking control mAb is defined as 100%) (mean ± SEM). (F-H) Intravital analyses. Human granulocytes were fluorescently labeled with TAMRA and pre-treated either with control antibody or anti-Siglec-9 mAb. Subsequently, the cells were injected into VAP-1 KOTG mice and their interaction with the inflamed vessel wall was analyzed using intravital microscopy, (F) The graph indicates the percentage of rolling cells, calculated from the total number of cells appearing during the observation period. (G) The plots show the velocity of rolling cells. Each dot represents the mean rolling velocity of a single cell. (H) The graph indicates the percentage of the cells that arrest on the venular wall for ≥ 30 s, calculated from the total number of rolling cells. In all three graphs the horizontal lines indicate mean values. The number of mice/venules/PMN bolus injections were 3/6/10 for control mAb and 3/8/11 for anti-Siglec-9 mAb (F-H). $*P < 0.05$; $**P < 0.01$; $***P < 0.001$, SSC-H = side scatter, FSC-H = forward scatter, MFI = mean fluorescence intensity after subtracting the MFI obtained from the stainings with the negative control antibody.

Europe PMC Funders Author Manuscripts

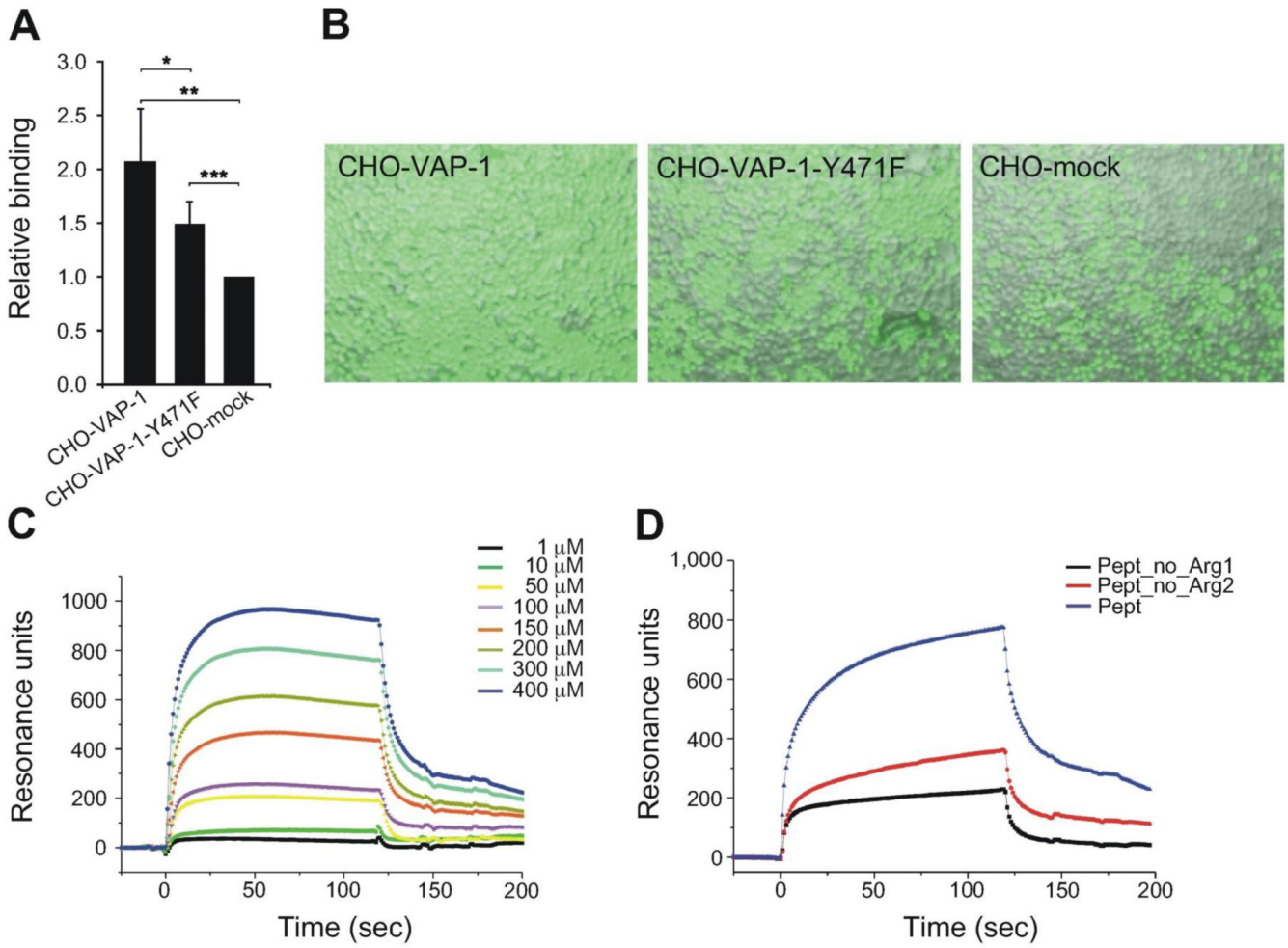

Figure 3. Interaction between Siglec-9 and VAP-1 involves both enzyme activity dependent and independent mechanisms

(A) Binding of CFSE labelled CHO-Siglec-9 transfectants to CHO cells expressing wild type VAP-1 (CHO-VAP-1), or the enzymatically inactive VAP-1 (CHO-VAP-1Y471F) and to mock transfected controls (CHO-mock). Binding is expressed as relative binding (mean ± SD, n = 5). **P* < 0.05; ***P* < 0,01; ****P* < 0.001. (B) Fluorescence microscopy images of the binding are shown as indicated. (C) Surface plasmon resonance analyses of the cyclic wild type Siglec-9-like peptide at different concentrations (0-400 μM). (D) An example of surface plasmon resonance analyses with the wild type and the mutated Siglec-9-like peptides. Three experiments were performed with comparable results. Arg 1 = Arg 284 and Arg 2 = Arg 290, Pept = wild type peptide.

Europe PMC Funders Author Manuscripts

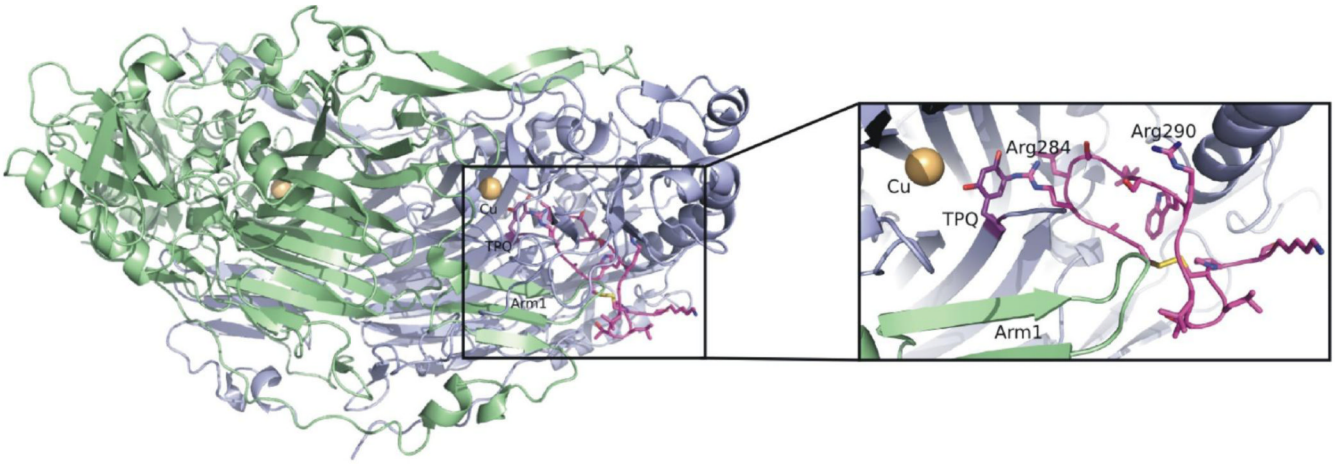

Figure 4.

Interaction of VAP-1 with the cyclic peptide CARLSLSWRGLTLCPSK (residues 283-297) **of Siglec-9**

The 3-dimensional structure of VAP-1 (monomer A, green; and monomer B, blue) with the peptide (pink) derived from Siglec-9 docked into the active site of the monomer B. The close up view shows that the docked peptide fits well into the active site of VAP-1. Arg284 and Arg290 in the docked peptide are labelled and Arg284 is covalently bound to topaquinone (TPQ; purple), which is in the active conformation. The figure was created with PYMOL Molecular Graphics System (DeLano Scientific).

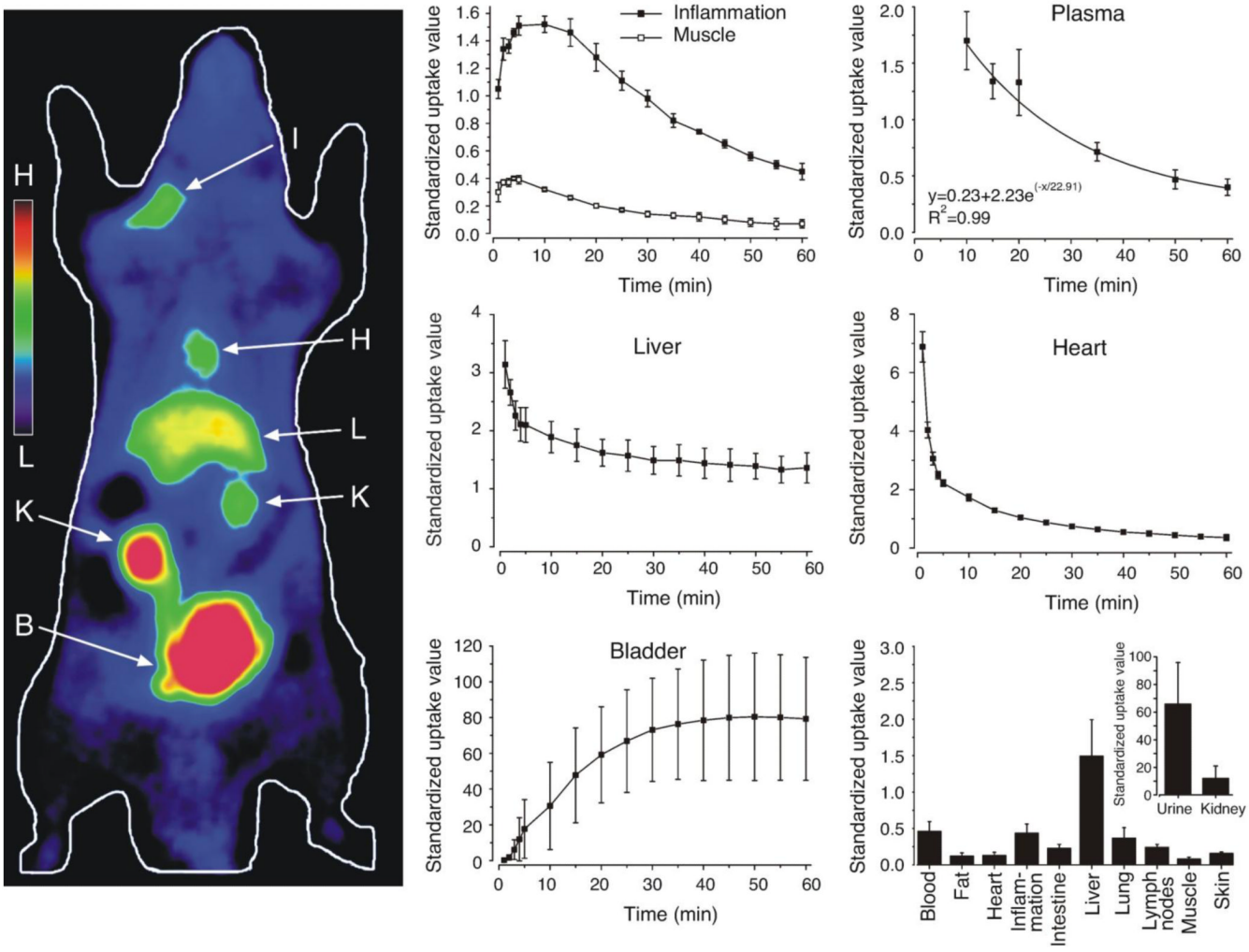

Figure 5. Siglec-9 peptide detects inflammation in PET

A representative whole-body coronal PET image of a rat intravenously injected with a ^{68}Ga-DOTA-peptide. Radioactivity uptake is clearly seen at the site of inflammation (I) but not in the surrounding muscle. In the PET image also the heart (H), the liver (L) and the urinary tract (kidney (K) and bladder (B)) are seen. Mean time-activity curves of three animals from the site of inflammation, muscle, liver, bladder, plasma and heart as well as standardized uptake values (SUV) obtained by PET imaging and ex vivo measurements 60 min post injection are presented on the right.

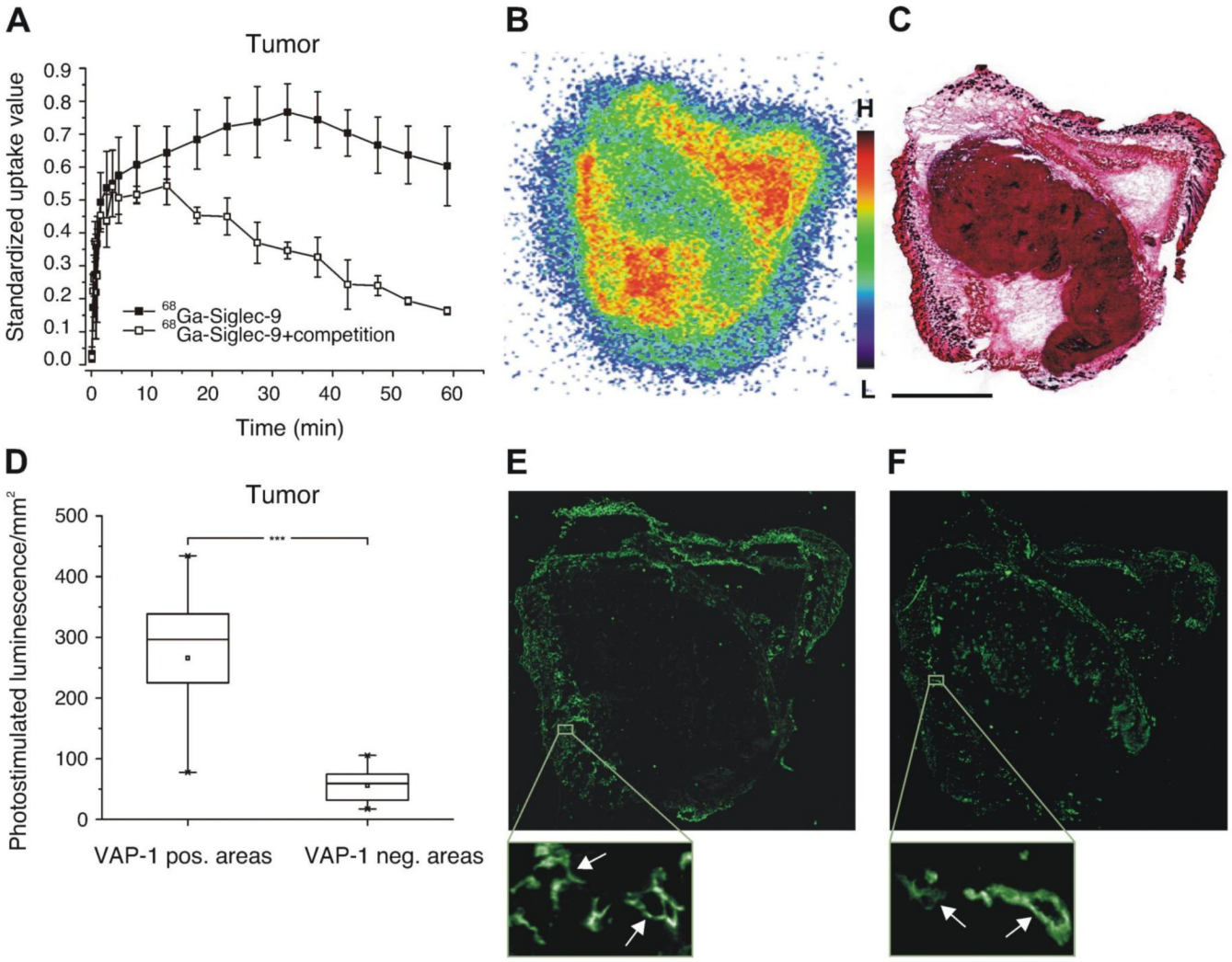

Figure 6. Siglec-9 peptide specifically targets VAP-1 in tumors

(A) Mean time-activity curves of ^{68}Ga-DOTA-peptide in a tumor xenograft obtained from PET imaging of wild-type mice (WT, black squares) and after competition with excess of the unlabeled peptide (open squares). (B) A representative image of autoradiography i.e. distribution of radioactivity in a tissue section and (C) hematoxylin-eosin staining of the section. (D) Combined results from autoradiography analyses of ^{68}Ga-DOTA-peptide distribution in melanoma xenografts of four mice at 15 min after i.v. injection presented as photostimulated luminescence (mean ± SD). Radioactivity was analyzed in VAP-1 negative and positive areas. (E) Immunohistochemical staining of the section of the same tumor as in b and c with anti-mouse VAP-1 antibody and (F) with anti-PV-1 antibody showing the blood vessels. Scale bar 2.5 mm for the whole tumor sections. In zoom-in insets individual VAP-1 and PV-1 positive tumor vessels are shown (arrows).

Europe PMC Funders Author Manuscripts

Table 1

Ex vivo biodistribution of ^{68}Ga-DOTA-peptide in VAP-1 positive wild type mice and VAP-1 negative knockout mice bearing melanoma xenografts

	WT 60 min	WT 60 min + KO 60 min Competition	
Blood	1.04 ± 0.44 *	0.20 ± 0.02	0.25 ± 0.01
Kidney	5.10 ± 0.86	6.39 ± 1.19	7.78 ± 1.47
Liver	1.82 ± 0.25	0.74 ± 0.08	0.97 ± 0.07
Lung	0.69 ± 0.21	0.15 ± 0.01	0.02 ± 0.00
Muscle	0.21 ± 0.07	0.03 ± 0.00	0.04 ± 0.01
Small intestine	0.59 ± 0.16	0.10 ± 0.03	0.08 ± 0.01
Tumour	0.56 ± 0.12	0.17 ± 0.02	0.20 ± 0.02

WT, VAP-1 positive wild-type mice; KO, VAP-1 negative knock-out mice. Results are expressed as standardized uptake values (mean ± SD; WT n = 3, WT + peptide competition n = 3, KO n = 2). Competition was done by injecting 500-fold molar excess of unlabeled DOTA-peptide along with ^{68}Ga-DOTA-peptide.

* Note that the relatively high level of radioactivity in the blood of WT mice is due to the soluble, enzymatically active VAP-1 in serum.